Evaluation of Spatial Resolution of a PET scanner through the simulation and experimental measurement of the Recovery Coefficient

E. Prieto, J.M. Martí-Climent, J. Arbizu, P. Garrastachu, I. Domínguez, G. Quincoces, M.J. García-Velloso, P. Lecumberri, M. Gómez-Fernández, and J.A. Richter

Abstract

Purpose: In order to measure spatial resolution of a PET tomograph in clinical conditions, this study describes and validates a method based on the recovery coefficient, a factor required to compensate underestimation in measured radioactivity concentration for small structures.

Methods: In a PET image, the recovery factors of radioactive spheres were measured and their comparison with simulated recovery coefficients yielded the tomographic spatial resolution. Following this methodology, resolution was determined in different surrounding media and several conditions for reconstruction, including clinical conditions for brain PET studies. All spatial resolution values were compared with those obtained using classical methods with point and line sources.

Results: In each considered condition, spatial resolution of the PET image estimated using the recovery coefficient showed good agreement with classical methods measurements, validating the procedure.

Conclusion: Measurement of the recovery coefficient provides an assessment of tomographic spatial resolution, particularly in clinical studies conditions.

Keywords: Point spread function; positron emission tomography; recovery coefficient; spatial resolution.

1. Introduction

Image formation on positron emission tomography (PET), as well as on any other linear imaging system, is completely described by its point spread function (PSF), generally dependent on spatial coordinates [1]. Under the assumption of spatial invariance, one PSF is defined for the complete field of view and the final image can be modelled as the real radioactivity distribution convolved by the PSF of the equipment.

The PSF determines spatial resolution of the imaging system, that is, its ability to distinguish between two objects in the formed image. The characterisation of spatial resolution consists in measuring the width of the point spread function, which is defined as its full width at half maximum (FWHM). Usually, it is obtained by imaging an object much smaller than the expected resolution and measuring its width in the final image.

The convolution with the PSF, as the PET image formation process, produces some smoothing that can result in an underestimation of the real radioactivity concentration, in addition to an overestimation of the object size. Thus, spatial resolution imposes a limitation not only for visual detection of small objects, but also for their accurate quantification [2]. This phenomenon is specially relevant in brain PET studies, because many brain structures are small and irregular [3]. To compensate for the decrease in measured radioactivity, a recovery coefficient (RC) is defined as the ratio between the observed concentration in the final image and the real radioactivity concentration [4]. Although the recovery coefficient concept has been extensively addressed in the literature [5], and its direct relation with spatial resolution has been previously described [6, 7], this relation has not been previously used for the estimation through mathematical adjustment of the resolution on image.

The objective of this study is to determine the effective tomographic spatial resolution for brain PET studies, through its influence on the underestimation of radioactivity concentration, measuring the recovery coefficients.

2. Methods

2.1 PET Tomograph

PET studies were performed using an ECAT EXACT HR+ tomograph (CTI/Siemens, Knoxville, Tennessee, USA). The system is composed of 4 rings with 72 detector modules, each with an 8 x 8 array of 4.39 mm x 4.05 mm x 30 mm bismuth germanate (BGO) crystals and coupled to four photomultiplier tubes [8]. Detectors are arranged as 32 crystal rings with inside diameter of 82.7 cm that generate 63 transaxial planes, covering an axial field of view of 15.5 cm. This tomograph uses three ^{68}Ge rotating rod sources for transmission scan acquisition.

All PET images presented in the following were acquired and reconstructed on a Sun Microsystems workstation with the ECAT v.7.1 software (CTI/Siemens, Knoxville, Tennessee, USA). Emission sinograms were acquired in 3D mode and corrected for random events. Reconstruction was performed using filtered backprojection including scatter correction, using brain mode and a zoom factor of 2.5. Three different sets of reconstruction parameters were used, defined by type and width of smoothing filter (FWHM) and matrix size. Specifically, used parameters were: (Hanning, 4.9 mm, 128 x 128), (Hanning, 4.9 mm, 512 x 512) and (Ramp, 2.0 mm, 512 x 512). First group of parameters corresponds to those used for clinical brain PET studies in our institution. When necessary, a 2D mode transmission scan was performed for attenuation correction after emission scan. Transmission image was segmented prior to the generation of the attenuation map by forward projection. This segmentation removes statistical errors in attenuation correction allowing the use of short transmission acquisition.

2.2 Evaluation of spatial resolution through the recovery coefficients

Spatial resolution was assessed evaluating its effect on the underestimation of radioactivity concentration for spherical objects. The method consisted of measuring the experimental RC in a PET image of radioactive spheres, simulating theoretical RC produced for several FWHM, and finding the resolution value that yielded the best fit between theoretical and experimental values.

The experiment was performed using a cylindrical Jaszczak phantom (Data Spectrum Corporation, Chapel Hill, North Carolina, USA) of 21.6 cm in diameter and 18.6 cm in height, containing six hollow spheres inserted at a radial position r = 57 mm, with diameters ranging from 7.9 mm to 24.8 mm.

Simulated recovery coefficients

Recovery coefficients can be estimated theoretically for specific geometric conditions by mathematical modelling. In this case, a phantom containing 6 spherical objects, with the same diameters as the spheres of the Jaszczak phantom, was simulated with a Matlab algorithm (Matlab 7.1, Mathworks Inc., Natick, Massachusetts, USA). These spheres were convolved with a 3-dimensional isotropic gaussian PSF, using different values of FWHM. Theoretical RC for each sphere was estimated as ratio between the maximum value after convolution and the initial value. Thus, a curve was obtained for each FWHM, representing the RC as a function of sphere diameter.

Experimental recovery coefficients

The six spheres were filled with a homogenized ^{18}F-FDG solution of 49.8 kBq/cm^3 at scanning time, that represents approximately the concentration of the higher uptake regions in brain tissue. The Jaszczak phantom with the radioactive spheres was scanned centered in the field of view. Several acquisitions were performed shifting axial position along 6 mm with 1 mm steps in order to account for different positions relative to tomographic rings. The protocol consisted in a 20 minutes 3D mode emission scan and a 5 minutes 2D mode transmission scan for attenuation correction. Different sets of reconstruction parameters were used. Afterwards, the experiment was repeated using the cylindrical phantom filled with non radioactive water, to account for the broadening of the point spread function associated with Compton scattering (spheres concentration: 51.9 kBq/cm^3).

For each sphere, the RC was estimated as the ratio of the maximum concentration measured in PET image and the real concentration. Average and standard deviation of recovery coefficient across considered axial positions was calculated. To avoid any bias due to attenuation and scattering corrections, values were normalised to the recovery coefficient of the greatest sphere, where no underestimation is expected.

Adjustment between theoretical and experimental recovery coefficients

The effective resolution was subsequently estimated as the FWHM value used in the theoretical model that best fitted the experimental values. Goodness of fit between theoretical curves and experimental values was assessed with a Pearson's chi-square test, which consisted in estimating the chi-square parameter and finding its minimum value.

This method was repeated to estimate spatial resolution in each considered axial position. System resolution for a given surrounding medium and reconstruction protocol was defined as the average value between resolution values obtained for all axial positions.

2.3 Classical spatial resolution measurement methods

Measurement of resolution with a point source

A 1.7 MBq ^{22}Na point source (model GF-0227, Isotope Product Laboratories, Valencia, CA, USA) with a 0.5 mm diameter, embedded in a plastic disk measuring 25 mm in diameter and 5 mm in height, was used to measure resolution. The point source was centred in the axial direction supported in the air by a plastic ruler at the position x = 0 mm, y = -57 mm. The source was moved in the axial direction with 1 mm steps along 15 mm. Acquisition time of

emission scan was 1 minute at each location. The sinogram was reconstructed without attenuation correction and using previously mentioned sets of reconstruction parameters.

Point source was also measured surrounded by water, using the Jaszczak phantom. Taking into account results in the previous experiment, in which variation of spatial resolution with source position was periodic, point source was shifted in 1 mm steps only along 6 mm. Acquisition time was 5 minutes for each emission scan and 5 minutes for each transmission scan. Reconstruction was performed with attenuation correction and using the same sets of parameters.

FWHM in radial, tangential, and axial directions were evaluated according to National Electrical Manufacturers Association (NEMA) standards [9]. Thus, radioactivity profile width was measured in resulting images, after linear interpolation between voxels value. Measurements were not corrected for source dimensions or positron range.

Measurement of resolution with a line source

A PET study of a 9.2 MBq ^{68}Ge line source encased in a sealed stainless steel rod (model LS-HR+, Isotope Product Laboratories, Valencia, CA, USA) was performed. The source was 183 mm length and had an inside diameter of 1.52 mm. The source was positioned parallel to the axial axis of the tomograph, at coordinates x = 0, y = -57 mm. The source was imaged both suspended in air and surrounded by water, using the Jaszczak phantom previously mentioned. Acquisition time for emission scan was 5 minutes. Reconstruction was performed using the three sets of parameters. When the phantom was filled with water, a 5 minutes transmission scan was also performed and attenuation correction was included.

Resolution was estimated perpendicularly to the line source position, that is radially and tangentially, as the width of the profiles extracted from the reconstructed 3D image, following NEMA standards [10]. Resolution values obtained for the 28 central planes were averaged to get the mean image resolution. Measurements were not corrected for source dimensions or positron range.

2.4 Application of RC method to other clinical protocols.

Once the methodology has been validated for a specific case (our brain protocol in the HR+ tomograph), it can be used to estimate effective resolution in any clinical protocol of interest. As an example, the recovery coefficient was used for estimation of resolution in the whole body protocols in our PET facility: a) acquisition in a Siemens HR+ tomograph with iterative reconstruction (2 iterations, 8 subsets) using a gaussian filter (FWHM=6 mm), a matrix size of 128x128 and a

zoom factor of 1; and b) acquisition in a Siemens Biograph 2 PET/CT tomograph with iterative reconstruction (2 iterations, 8 subsets) using a gaussian filter (FWHM=5 mm), a matrix size of 128x128 and a zoom factor of 1.

3. Results

3.1 Measurement of spatial resolution through the recovery coefficients

Although all spheres were filled with the same radioactive solution, the maximum measured radioactivity concentration decreased as sphere size decreased. Table 1 shows the RC for each sphere and for each considered condition of acquisition and reconstruction. With regard to reconstruction parameters, radioactivity concentration, and consequently recovery coefficients, increased with the matrix size and the use of a ramp filter.

Curves representing simulated recovery coefficients as a function of object size were calculated for different FWHM values. Some of these curves are represented in Fig. 1. These theoretical curves show that the minimum size of spheres that can be measured without underestimation, admitting errors of less than 2 %, is 2.7 times the FWHM, as has been shown by others [2].

The minimisation of the chi-square parameter for each acquisition and reconstruction condition is graphically shown in Fig. 2. The minimum chi-square yielded the spatial resolution that produces the best adjustment between theoretical and experimental data (Table 1). In the case of clinical conditions for brain studies (acquisition in water and reconstruction with first group of parameters), best fit was produced for a FWHM of 7.3 $\pm$ 0.1 mm (Fig.2).

3.2 Classical spatial resolution measurement methods

Measurement of resolution with a point source

For each acquisition condition and each group of reconstruction parameters, resolution values were measured in different axial positions to calculate mean value in the sampled axial field of view (Table 2). The average of axial, radial and tangential values is also shown, providing a measure of the effective 3-dimensional resolution. The best spatial resolution value, obtained for the source suspended in air, and reconstructed with the finest matrix size (512 x 512) and the sharpest filter (Ramp filter), was 4.76 $\pm$ 0.15 mm. However, in conditions of clinical brain studies, that is, source surrounded by water and image reconstructed with matrix size of 128 x 128 and a Hanning filter, resolution degrades to 7.27 $\pm$ 0.02 mm, corresponding to the worst value.

Variation of spatial resolution with axial position was examined when point source was acquired in air (Fig. 3 shows this variation for the brain reconstruction parameters). The transverse components were unvarying with source position, contrary to axial resolution, which changed significantly showing an opposite variation with maximum voxel value measured in reconstructed image (Fig. 3). This variation was periodic with a local maximum resolution value appearing approximately each two 1 mm shifts (voxel size is 2.45 mm). In the coronal view, this difference in measured FWHM can be noticed directly on image, as a variation in observed object size (Fig. 4).

Measurement of resolution with a line source

Spatial resolution values represented in Table 3 were obtained using the ^{68}Ge line source in different conditions of acquisition and reconstruction. Spatial resolution at r = 57 mm in conditions equivalent to those of brain studies was 7.67 ± 0.25 mm. Best spatial resolution value was 5.08 ± 0.05 mm (5.17 ± 0.02 mm in radial direction and 4.99 ± 0.03 mm in tangential drection). This value was obtained when the source was acquired in air and the image reconstructed with maximum matrix size and the sharpest filter.

3.3 Application of RC method to other clinical protocols.

The developed methodology for spatial resolution measurement was repeated for the other acquisition protocols. The adjustment of the theoretical and experimental RC values yielded resolution values of 7.7 mm and 9.3 mm for the whole body protocols in the Siemens HR+ and in the Siemens Biograph 2 PET/CT respectively.

4. Discussion

Different experiments were carried out to determine tomographic resolution. First, resolution was estimated through the recovery coefficients of spherical objects. In order to validate obtained results, resolution was measured classically as the width of radioactivity distribution profile obtained from a point source and a line source. In addition, these values were similar to previous published data [8].

Our interest in assessing spatial resolution from the recovery coefficients resides in the fact that it is a direct measurement of the degradation produced by the limited spatial resolution on the final PET image, especially in clinical conditions.

Estimations of tomographic FWHM have been widely used for recovery coefficients calculation [11]. We propose the inverse process, that is, the evaluated recovery coefficients can provide the effective spatial resolution on final image.

4.1 Advantages of spatial resolution measurement through the RC

Classical methods for spatial resolution measurement consist in measuring the width of the radioactivity distribution profile of a point or line source on final image. According to NEMA standards [12], intended for the characterisation of PET scanners, for an accurate estimation of spatial resolution from profiles of reconstructed data, voxel dimensions should be one-tenth the expected FWHM, allowing the interpolation of at least ten points. This condition is not satisfied for resolution measurement with point and line sources using clinical reconstruction protocols. In the axial direction, sampling is limited by the number of detector rings and for the Siemens HR+ tomograph axial sampling is 2.425 mm. Given that estimated FWHM is in a range from 5 to 8 mm, axial spatial resolution must be estimated by interpolation of 2 or 3 points, which does not satisfy the NEMA requirement. Besides, a transverse matrix size of 128 x 128 and a zoom factor of 2.5, used in clinical brain PET studies in our institution, correspond to a pixel size of 2.056 mm x 2.056 mm, with which the spatial resolution is estimated from 3 or 4 points. The case is even worse for the whole body protocol, where a matrix size of 128 x 128 and a zoom factor of 1 yield a voxel size of 5.148 mm x 5.148 mm. Then, in clinical conditions sampling in the transverse directions neither is enough for resolution estimation with standard procedures [12].

Therefore, spatial resolution measurement for a specific clinical protocol using either a point or line source would require changing the standard matrix for a finest one, in order to have enough sampling for data interpolation. However, the resolution value with this fine sampling would not exactly correspond to the observed with the real coarse sampling in clinical conditions.

However, the assessment of spatial resolution from the recovery coefficients does not require any data interpolation and consequently it can be applied for any voxel size, including clinical conditions.

In this study, the objective was to validate the RC model for spatial resdution measurement and validation was performed in a specific case (custom brain PET protocol in the HR+ tomograph). Once this methodology has been validated, it can be applied to any other acquisition protocol (other tomographs, different radionuclides, 2D or 3D acquisition...). In order to show the applicability of the RC method, it was applied to other two situations (whole body in the HR+ PET tomograph and whole body in the Biograph 2 PET/CT tomograph).

4.2 Acquisition and reconstruction conditions

Acquisition was done in two conditions, with the sources surrounded by air and by water. In PET studies, brain tissue itself produces attenuation and scattering of annihilation photons, so the experiment with water reproduces better the brain acquisition conditions. The attenuation and scattering effect of the surrounding media may degrade spatial resolution value. This degradation is observed in a minor difference between FWHM measured in air and water with the point and line sources. However, this effect is not noticed in the spheres where spatial resolution seems to be slightly better. The fact is related to an error in attenuation correction for spheres in air. In this case, the segmentation of the transmission image to obtain the attenuation map assigned a wrong attenuation coefficient to air inside the Jaszczak phantom (approximately 0.01 cm^{-1}). Although spheres uptake values had been normalized to eliminate the possible bias due to this type of errors, it have not been effective enough to remove the bias in the resolution estimation.

Different reconstruction parameters were used because spatial resolution of reconstructed image depends, not only on physical and geometrical factors for a particular system design ($FWHM_{system}$), but also on the method and parameters used for reconstruction. In fact, a reasonable accurate estimate of final spatial resolution has been reported to be:

$$FWHM = K_{reconstruction} \cdot FWHM_{system}$$

where $FWHM_{system}$ depends on the detector size (d), photon non-collinearity (related to the tomograph diameter D), positron range (r), and the contribution of a block decoding scheme (b),

$$FWHM_{system} = \sqrt{\left(\frac{d}{2}\right)^2 + (0.0022 \cdot D)^2 + r^2 + b^2}$$

For this reason, different reconstruction parameters were used, including those proposed by NEMA for evaluation of resolution, that is a ramp filter with cut-off at Nyquist frequency [9], and a fine matrix size. Trying to simulate brain studies conditions, custom brain reconstruction parameters in clinical practice were used (128 x 128 matrix size and Hanning filter with FWHM = 4.9 mm). Reconstruction with an intermediate condition explains the influence of each modified parameter.

In all experiments, resolution becomes better as the sampling increases and the smoothing decreases. The width and type of filter have been shown to be the most critical factors.

4.3 Radioisotopes

For the measurement of spatial resolution by means of the recovery coefficients, spheres were filled with ^{18}F, which is the most frequently used radioisotope in PET for clinical studies.

However, for the measurement of resolution with point and line sources, other radioisotopes were used, as has been done by others [14]. The reason is that embedded sources with long half-life radioisotopes, suitable for scanner characterisation and control purposes, are commercially available.

The point source was a ^{22}Na source, which has a similar positron emission energy (E_{avg} = 0.216 MeV) to ^{18}F (E_{avg} = 0.250 MeV) and, thus, similar positron range [15].

A line source of ^{68}Ge was used, with positron emission energy of 0.836 MeV [15], considerably higher than that of ^{22}Na. Therefore, positron range resolution degradation is higher and spatial resolution values obtained with the line source were, in general, higher than those obtained with the point source.

4.4 Invariance of the PSF

PET tomographs are linear systems, but not spatially invariant, that is, the characteristics of the PSF depend on the spatial position. However, measurements were carried out at a specific radial position. Due to the fact that the Jaszczak phantom allows to place six spheres at r = 57 mm, this radial position was selected for the measurements. Besides, this is an intermediate position between the tomograph axis and the radius of a human head. Then, estimated resolution would be representative for the considered field of view in brain PET studies.

Variance of PSF through the axial direction was considered. In fact, this variation has been evaluated using the point source. The relationship between resolution and maximum voxel value showed that their variation depends on the position of the source in relation to the tomographic planes. Therefore, minimum FWHM was measured when the source was centred in an axial plane and maximum when it was positioned between two consecutive planes (Fig. 2).

Due to this axial variation, spatial resolution was measured in several axial positions, considering the average of all measurements as the effective resolution. Thus, the behaviour of the system was actually characterised by one PSF and one resolution value.

4.5 Isotropic PSF

Using the point and line sources, the anisotropic characteristic of the tomographic resolution is observed (Tables 2,

3). However, for the estimation of spatial resolution via the recovery coefficients, an isotropic gaussian PSF was assumed in the theoretical model, as has been done in other works for the evaluation of the recovery coefficients [16]. In fact, due to the spherical symmetry of the modeling used in this work, if σ_x, σ_y and σ_z of the Gaussian PSF were treated as different unknown factors, there would be several solutions for the problem.

Besides, underestimation in measured radioactivity is due to the combination of the three directional spatial resolution values, and the estimated isotropic FWHM represents an effective value with regard to the influence in the recovery coefficient.

5. Conclusions

Spatial resolution has been evaluated using different radioactive sources and different conditions. Reconstruction parameters have been shown to have a great influence in final resolution, the type and width of smoothing filter being the most critical parameters.

The method for spatial resolution measurement based on the recovery coefficient has been validated by comparison with classical methods. Line and point sources gave appropriate values for spatial resolution by measuring radioactive profile width when there was enough sampling, which is the case at PET scanner performance characterisation. When resolution must be measured in clinical conditions, recovery coefficients produced more representative values of resolution without mentioned limitation for sampling.

The obtained spatial resolution for the EXACT ECAT HR+ PET tomograph working in our clinical conditions for brain studies (matrix size of 128 x 128, a zoom factor of 2.5 and a Hanning filter with FWHM = 4.9 mm) was 7.3 mm. In fact, this method can be used for spatial resolution measurement in any reconstruction conditions.

Acknowledgment

The authors would like to acknowledge the staff of the Cyclotron Unit for radioisotope production and nuclear medicine technologists' support in acquiring the imaging.

References

1. J.M. Links, Advances in nuclear medicine instrumentation: Considerations in the design and selection of an imaging system, Eur.J.Nucl.Med. 25 (1998) 1453-1466.

2. R.M. Kessler, J.R. Ellis Jr, M. Eden, Analysis of emission tomographic scan data: Limitations imposed by resolution and background, J.Comput.Assist.Tomogr. 8 (1984) 514-522.

3. J.C. Mazziotta, M.E. Phelps, D. Plummer, D.E. Kuhl, Quantitation in positron emission computed-tomography .5. physical-anatomical effects, J.Comput.Assist.Tomogr. 5 (1981) 734-743.

4. E.J. Hoffman, S.C. Huang, M.E. Phelps, Quantitation in positron emission computed tomography: 1. Effect of object size, J.Comput.Assist.Tomogr. 3 (1979) 299-308.

5. C.H. Chen, Simultaneous recovery of size and radioactivity concentration of small spheroids with PET data, Journal of Nuclear Medicine 40 (1999) 118-130.

6. O.G. Rousset, Correction for partial volume effects in PET: Principle and validation, J.Nucl.Med. 39 (1998) 904-911.

7. T.R. Miller, Design and use of PET tomographs: The effect of slice spacing, J.Nucl.Med. 31 (1990) 1732-1739.

8. G. Brix, J. Zaers, L.E. Adam, M.E. Bellemann, H. Ostertag, H. Trojan, U. Haberkorn, J. Doll, F. Oberdorfer, W.J. Lorenz, Performance evaluation of a whole-body PET scanner using the NEMA protocol. National Electrical Manufacturers Association, J.Nucl.Med. 38 (1997) 1614-1623.

9. J.S. Karp, M.E. Daube-Witherspoon, E.J. Hoffman, T.K. Lewellen, J.M. Links, W.H. Wong, R.D. Hichwa, M.E. Casey, J.G. Colsher, R.E. Hitchens, Performance standards in positron emission tomography, J.Nucl.Med. 32 (1991) 2342-2350.

10. National Electrical Manufactures Association, NEMA standards publication NU 2-1994: Performance measurements of positron emission tomographs (1994)

11. M. Samuraki, I. Matsunari, W. Chen, K. Yajima, D. Yanase, A. Fujikawa, N. Takeda, S. Nishimura, H. Matsuda, M. Yamada, Partial volume effect-corrected FDG PET and grey matter volume loss in patients with mild Alzheimer's disease, Eur.J.Nucl.Med. 34 (2007) 1658-1669.

12. National Electrical Manufactures Association, NEMA standards publication NU 2-2001: Performance measurements of positron emission tomographs (2001)

13. G. Tarantola, F. Zito, P. Gerundini, PET instrumentation and reconstruction algorithms in whole-body applications, J.Nucl.Med. 44 (2003) 756-769.

14. Y.C. Tai, A. Ruangma, D. Rowland, S. Siegel, D.F. Newport, P.L. Chow, R. Laforest, Performance evaluation of the microPET focus: A third-generation microPET scanner dedicated to animal imaging, J.Nucl.Med. 46 (2005) 455-463.

15. M. Partridge, A. Spinelli, W. Ryder, C. Hindorf, The effect of ß+ energy on performance of a small animal PET camera, Nucl Instrum Meth A. 568 (2006) 933-936.

16. H.W. Muller-Gartner, J.M. Links, J.L. Prince, R.N. Bryan, E. McVeigh, J.P. Leal, C. Davatzikos, J.J. Frost, Measurement of radiotracer concentration in brain gray matter using positron emission tomography: MRI-based correction for partial volume effects, J.Cereb.Blood Flow Metab. 12 (1992) 571-583.

Figure legends

Fig. 1. Theoretical recovery coefficients for several FWHM and experimental values for brain PET conditions (Hanning filter, FWHM 4.9 mm, matrix 128 x 128).

Fig. 2. Minimization of chi-square parameter for the assessment of the spatial resolution.

Fig. 3. Spatial resolution and maximum voxel value on image, measured with the point source surrounded by air and positioned at different axial positions (clinical brain reconstruction parameters).

Fig. 4. Coronal view of PET image of point source in two different axial positions: (a) source centred in the plane; (b) source between two consecutive planes.

Table 1
Experimental recovery coefficients for spherical objects with different diameters (∅) and resulting spatial resolution by comparison with theoretical values

Medium	Matrix size	Filter type	Recovery coefficient						FWHM (mm)
			∅=24.8 mm	∅=19.8 mm	∅=15.4 mm	∅=12.4 mm	∅=9.9 mm	∅=7.9 mm	
Air	128 x 128	Hanning	1.00 ± 0.11	0.93 ± 0.11	0.81 ± 0.10	0.71 ± 0.09	0.51 ± 0.05	0.30 ± 0.03	7.7 ± 0.1
	512 x 512	Hanning	1.00 ± 0.11	0.93 ± 0.11	0.83 ± 0.11	0.75 ± 0.09	0.56 ± 0.05	0.35 ± 0.03	7.2 ± 0.1
	512 x 512	Ramp	1.00 ± 0.10	0.92 ± 0.10	0.83 ± 0.10	0.78 ± 0.10	0.66 ± 0.06	0.49 ± 0.04	6.4 ± 0.1
Water	128 x 128	Hanning	1.00 ± 0.02	0.96 ± 0.02	0.86 ± 0.01	0.74 ± 0.01	0.53 ± 0.01	0.33 ± 0.01	7.3 ± 0.1
	512 x 512	Hanning	1.00 ± 0.02	0.96 ± 0.02	0.88 ± 0.01	0.78 ± 0.01	0.59 ± 0.01	0.38 ± 0.01	6.9 ± 0.1
	512 x 512	Ramp	1.00 ± 0.07	0.96 ± 0.07	0.86 ± 0.04	0.80 ± 0.05	0.68 ± 0.05	0.51 ± 0.04	6.1 ± 0.2

Table 2
Spatial resolution obtained with a point source imaged surrounded by air and water and reconstructed with different parameters

Medium	Matrix size	Filter type	FWHM (mm)			
			Tangential	Radial	Axial	Average
Air	128 x 128	Hanning	7.09 ± 0.02	7.18 ± 0.03	6.91 ± 0.09	7.06 ± 0.04
	512 x 512	Hanning	6.36 ± 0.02	6.57 ± 0.03	6.89 ± 0.10	6.61 ± 0.04
	512 x 512	Ramp	4.63 ± 0.03	4.56 ± 0.06	5.08 ± 0.40	4.76 ± 0.15
Water	128 x 128	Hanning	7.57 ± 0.05	7.44 ± 0.05	6.80 ± 0.04	7.27 ± 0.02
	512 x 512	Hanning	6.48 ± 0.02	6.44 ± 0.02	6.83 ± 0.04	6.59 ± 0.02
	512 x 512	Ramp	4.63 ± 0.02	4.67 ± 0.04	4.92 ± 0.23	4.74 ± 0.09

Table 3
Spatial resolution obtained with a line source imaged surrounded by air and water and reconstructed with different parameters

Medium	Matrix size	Filter type	FWHM (mm)		
			Tangential	Radial	Average
Air	128 x 128	Hanning	7.69 ± 0.05	7.36 ± 0.02	7.52 ± 0.07
	512 x 512	Hanning	6.85 ± 0.01	6.78 ± 0.02	6.81 ± 0.03
	512 x 512	Ramp	5.17 ± 0.02	4.99 ± 0.03	5.08 ± 0.05
Water	128 x 128	Hanning	7.72 ± 0.13	7.63 ± 0.12	7.67 ± 0.25
	512 x 512	Hanning	6.87 ± 0.02	6.79 ± 0.03	6.83 ± 0.05
	512 x 512	Ramp	5.10 ± 0.06	5.07 ± 0.07	5.08 ± 0.13

FIGURE 1

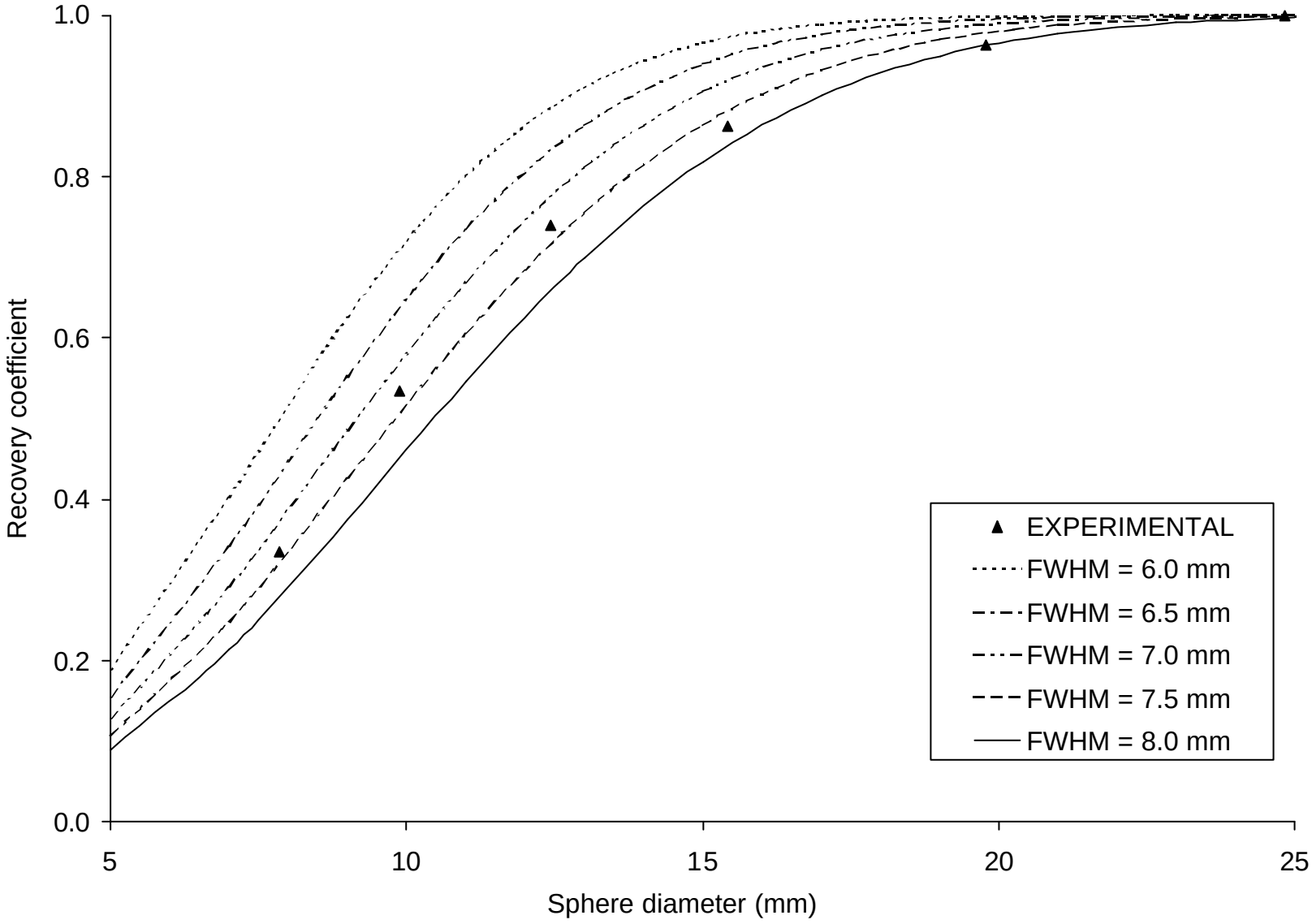
1.0
0.8
0.6
0.4
0.2
0.0
Recovery coefficient
5
10
15
20
25
Sphere diameter (mm)
EXPERIMENTAL
FWHM = 6.0 mm
FWHM = 6.5 mm
FWHM = 7.0 mm
FWHM = 7.5 mm
FWHM = 8.0 mm

FIGURE 2

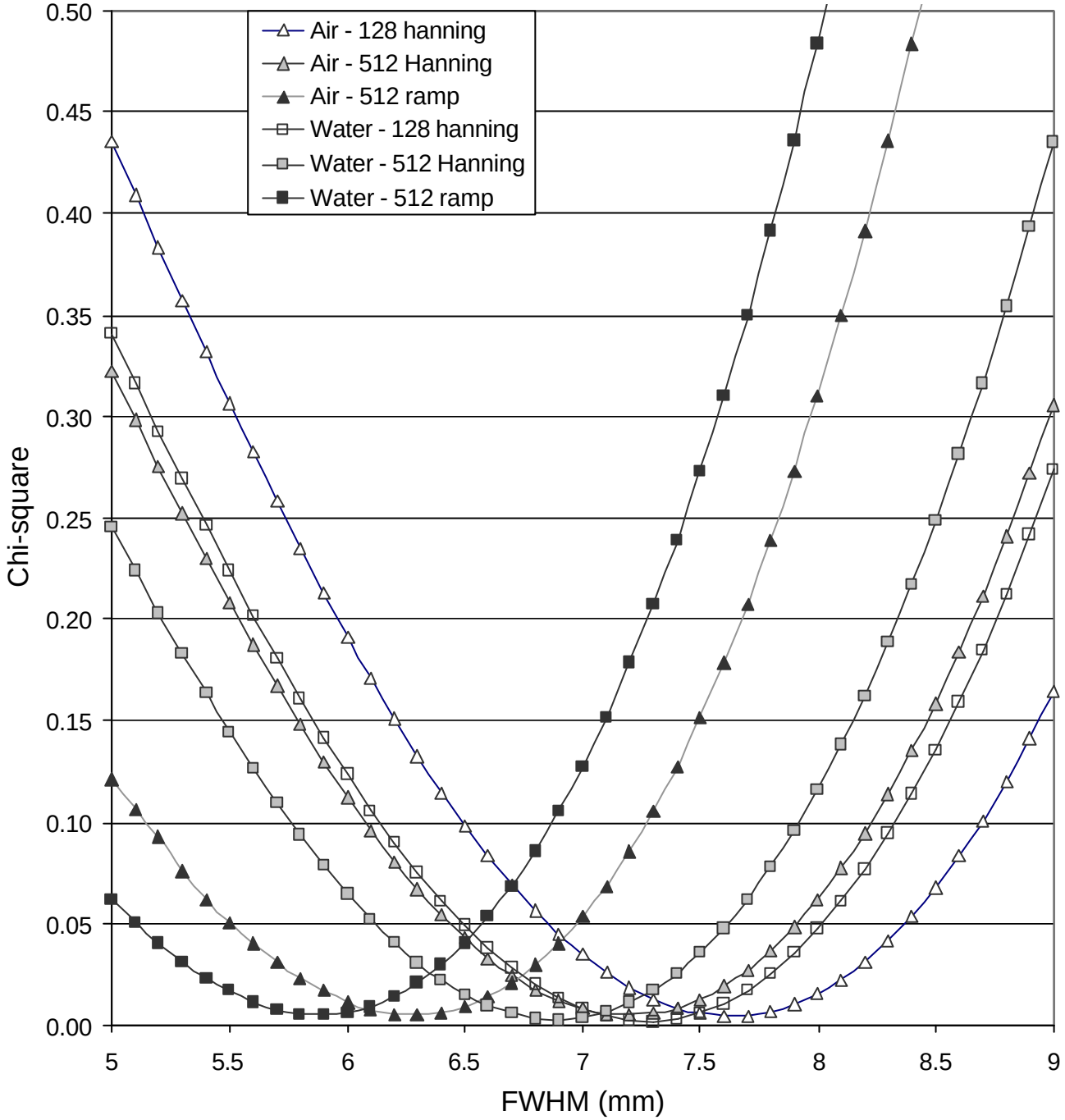
Air - 128 hanning
Air - 512 Hanning
Air - 512 ramp
Water - 128 hanning
Water - 512 Hanning
Water - 512 ramp
Chi-square
0.50
0.45
0.40
0.35
0.30
0.25
0.20
0.15
0.10
0.05
0.00
5
5.5
6
6.5
7
7.5
8
8.5
9
FWHM (mm)

FIGURE 3

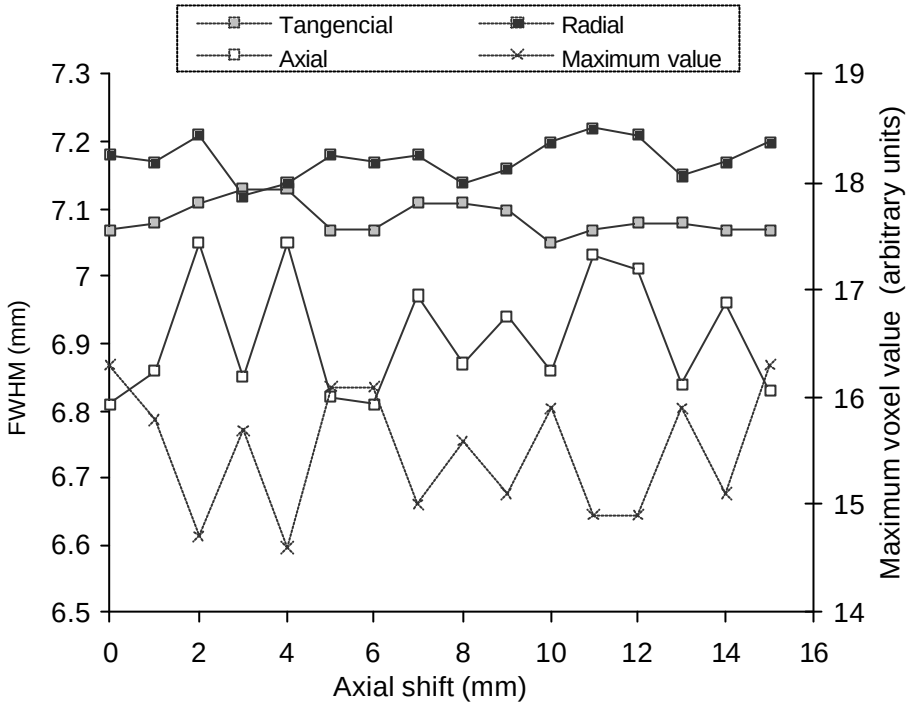
Tangencial
Radial
Axial
Maximum value
FWHM (mm)
Maximum voxel value (arbitrary units)
Axial shift (mm)
7.3
7.2
7.1
7
6.9
6.8
6.7
6.6
6.5
19
18
17
16
15
14
0
2
4
6
8
10
12
14
16

FIGURE 4